Prediction of Pore Water Pressure During Earthquakes in Southern Kyoto Area

F. Oka

Gifu University, Gifu, Japan

Prediction of Pore Water Pressure During Earthquakes in Southern Kyoto Area

F. Oka

Associate Professor, Department of Civil Engineering, Gifu University, Yanagido 1-1, Gifu, Japan

SYNOPSIS This paper is concerned with the liquefaction analysis for the hypothetical earthquake in southern Kyoto area in Japan. The method of liquefaction analysis can consider the local soil properties of sand and clay, using the constitutive equations of clay and sand, and the theory of mixture. From this study, it becomes evident that liquefaction will occur at the site near the river, and also liquefaction can be observed in the clay layers.

INTRODUCTION

This paper is concerned with the liquefaction analysis for the hypothetical earthquake in southern Kyoto area in Japan. Recently, it has been confirmed that the ground motion during the earthquake is greatly influenced by the local ground conditions near the surface. Therefore, it is necessary to take account of the local properties of geotechnical materials for earthquake response analysis.

Considering the problem mentioned above, the author developed the method of liquefaction analysis that can consider the local soil properties of sand and clay, using the constitutive equations of clay and sand, and the theory of two-phase mixture. This method was applied to predict the pore water pressure developed in the ground due to the hypothetical earthquake in Kyoto. From this study, it becomes clarified that liquefaction will occur at the site near the river, and also liquefaction can be observed even in the clay layers.

CONSTITUTIVE EQUATIONS OF SAND AND CLAY

Constitutive equation of sand

Oka and Washizu(1981) developed an elasto-plastic constitutive equation of sand and overconsolidated clay that can describe the behavior under cyclic loading. The proposed model is based on the newly developed plastic potential and the concepts of bounding surface and kinematic work-hardening. In this section, following Oka and Washizu(1981), a cyclic elasto-plastic constitutive theory of sand is summarized.

The boundary between the normally consolidated region and the overconsolidated region is defined as a boundary surface which is given by

$$f_b = \bar{\eta}^*_{(0)} + M^*_m \ln(\sigma'_m/\sigma'_{mb}) = 0 \qquad (1)$$

where σ'_m is a mean effective stress, σ'_{me} is equal to the preconsolidation pressure when soil is normally consolidated. $\bar{\eta}^*_{(0)}$ in Eq.(1) is a stress parameter that can represents the anisotropic concolidation history(Sekiguch and Ohta 1977), and defined by

$$\bar{\eta}^*_{(0)} = \{(\eta^*_{ij}-\eta^*_{ij(0)})(\eta^*_{ij}-\eta^*_{ij(0)})\}^{1/2} \qquad (2)$$

$$\eta^*_{ij} = s_{ij}/\sigma'_m \qquad (3)$$

$$\eta^*_{ij(0)} = (s_{ij}/\sigma'_m)_{(0)} \qquad (4)$$

where $\eta^*_{ij(0)}$ is a value of η^*_{ij} at the end of anisotrpic consolidation and s_{ij} is a deviatoric stress tensor. M^*_m is a value of $(\eta^*_{ij}\eta^*_{ij})^{1/2}$ when maximum cpmpression of the material takes place.
The yield function is given by

$$f = \bar{\eta}^* - \bar{\eta}^*_y = 0 \qquad (5)$$

in which $\bar{\eta}^*$ is a relative stress parameter that describes the kinematical hardening.

$$\bar{\eta}^* = \{(\eta^*_{ij}-\eta^*_{ij(n)})(\eta^*_{ij}-\eta^*_{ij(n)})\}^{1/2} \qquad (6)$$

In this equation, $\eta^*_{ij(n)}$ is the value of η^*_{ij} at the n-th times turning over point of loading direction.
The plastic potential function f_p is assumed to be given by

$$f_p = \bar{\eta}^* + \tilde{M}^* \ln(\sigma'_m/\sigma'_{m(n)}) = 0 \qquad (7)$$

Subscript (n) denotes the value at the n-th times turning over point of loading direction.
The parameter $\tilde{M}^*$ is given by

$$\tilde{M}^* = -\frac{\eta^*}{\ln(\sigma'_m/\sigma'_{mc})} \qquad (8)$$

$$(\eta^* = (\eta^*_{ij}\ \eta^*_{ij})^{1/2}$$

In the region $f_b > 0$, i.e., in the normally consolidated region, $\hat{M}^*$ and σ'_{mc} varies according to the following rule.

$$\sigma'_{mc} = \sigma'_{me} \exp(\eta^*/M^*_m) \quad (9)$$

In the overconsolidated region, we keep $\hat{M}^* = M^*_m$ after the value of $\hat{M}^*$ attains to the value of M^*_m. The plastic strain increment tensor $d\varepsilon^p_{ij}$ is given by the following non-associated flow rule as

$$d\varepsilon^p_{ij} = \frac{\partial f_p}{\partial \sigma'_{ij}} df \quad (10)$$

where σ'_{ij} is an effective stress tensor and the papameter Λ can be determined by the following hardening function.

$$\bar{\gamma}^* = \frac{\bar{\gamma}^*(M^*_f + \eta^*_{(n)})}{G'(M^*_f + \eta^*_{(n)} - \bar{\eta}^*)} \quad (11)$$

In Eq.(11), $\bar{\gamma}^*$ is called relative plastic deviatoric strain given by

$$\bar{\gamma}^* = \{(e^p_{ij} - e^p_{ij(n)})(e^p_{ij} - e^p_{ij(n)})\}^{1/2} \quad (12)$$

where e^p_{ij} is a plastic deviatoric strain tensor.

G' is the initial tangent modulus of $\bar{\gamma}^* - \bar{\eta}^*$ curve, M^*_f is the value of η^* at the failure state and subscript (n) denotes the n-th turning over point of loading direction.

Taking account of elastic component of strain increment, total strain increment is obtained as

$$d\varepsilon_{ij} = \frac{1}{2G} ds_{ij} + \frac{\kappa}{(1+e)\sigma'_m} d\sigma'_m \frac{1}{3}\delta_{ij} + d\varepsilon^p_{ij} \quad (13)$$

where G is an elastic shear modulus and κ is a swelling index.

Constitutive equation of normally consolidated clay

As for the constitutive equation of normally consolidated clay, the elasto-viscoplastic constitutive equation proposed by Oka(1981) and Adachi and Oka(1982) is used.
The elasto-viscoplastic constitutive equation of normally consolidated clay(Adachi and Oka 1982) is written by

$$\dot{\varepsilon}^{vp}_{ij} = \frac{1}{2G}\dot{s}_{ij} + \frac{\kappa}{3(1+e)\sigma'_m}\dot{\sigma}'_m \delta_{ij}$$

$$+ \langle\Phi(F)\rangle \frac{\partial f_d}{\partial \sigma'_{ij}} \quad (14)$$

$$\langle\Phi(F)\rangle = CM^*\sigma'_m \exp(m' \ln(\sigma'_m/\sigma'_{me}) + m'\bar{\eta}^*_{(0)}/M^*$$

$$- m'(1+e)v^p/(\lambda - \eta)) \quad (F \geq 0)$$

$$= 0 \quad (F < 0) \quad (15)$$

$$F = (f_d - \kappa_s)/\kappa_s \quad (16)$$

f_s denotes the static yield function. Since F=0 denotes the static yield function (Perzyna 1983), f_d is given by

$$f_d = \bar{\eta}^*/M^* + \ln(\sigma'_m/\sigma'_{md}) = 0 \quad (17)$$

It is assumed that static yield function is expressed by

$$f_s = \bar{\eta}^*/M^* + \ln(\sigma'_m) = \ln(\sigma'^{(s)}_{my}) \quad (18)$$

In Eqs.(14)-(18), λ is a consolidation index, κ is a swelling index, M^* is the value of η^* at critical state, C and m' are viscoplastic parameters and v^p is a plastic volumetric strain.

Because of the numerical restriction, the following failure conditions are introduced.

$$|\varepsilon^p_{12}| \geq 0.05 \quad (19) \qquad \sigma'_m \leq 0.05\sigma'_{m(0)} \quad (20)$$

where $\sigma'_{m(0)}$ is an initial value of σ'_m.

After failure, the constitutive equation of soil is replaced by the bilinear stress-strain relation.

$$\sigma'_{12} = 2G\varepsilon_{12} \quad (|\sigma'_{12}| \leq \sigma'_{12y})$$
$$\sigma'_{12} = 2\bar{G}\varepsilon_{12} \quad (|\sigma'_{12}| > \sigma'_{12y}) \quad (21)$$

$$\bar{G} = 5\text{kgf/cm}^2, \quad \sigma'_{12y} = 0.05 \text{ kgf/cm}^2$$

LIQUEFACTION ANALYSIS

Oka and Sekiguchi(1980) and Oka,Sekiguchi and Goto(1981) developed a method of liquefaction analysis of sand deposits by using an elasto-plastic constitutive equation. Oka and Murase (1980)performed the liquefaction analysis of sand depositt using the cyclic elasto-plastic constitutive equation by Oka and Washizu (1981). Oka and Hibi(1982) carried out the liquefaction analysis of saturated ground composed of sands and clays.

In this section, we will use the method by Oka and Sekiguchi(1981) and Oka and Hibi(1982). The one-dimensional approximated equation of motion for solid phase and kinematic equations are used. For fluid phase, we neglect the acceleration term in the equation of motion. We assume that horizontal strain is zero. The finite differenace method and the method of characteristics are used for solving the partial differential equations.

Ground model

Table I shows the soil parameters profile at three sites in Kyoto southern area(Fig.1). The N-value(blow count) distribution were obtained by Kobori(1978). The soil parameters are determined as follows from N-values.

1) Void ratio e

$$\varphi'=0.3N + 27 \tag{22}$$

$$e= 0.55/\tan\varphi' \tag{23}$$

where N is a value of blow count and φ' is an internal friction angle.

2) Elastic shear modulus G

Mass density of soil is determined by Table II, and elastic shear wave velocity is calculated by the following formula.(Okubo et al. 1974)

$$V_s = \begin{cases} 98.9\ N^{0.35}\text{(clay)} \\ 68.7\ N^{0.41}\text{(sand)} \\ 88.2\ N^{0.34}\text{(gravel)} \end{cases} \tag{24}$$

Elastic shear modulus is determined by the value of V_s and mass density as follows.

$$G=\rho Vs^2 \quad (\rho\text{:mass density}) \tag{25}$$

3) Coefficient of permeability
Coefficient of permeability is predicted from Table III.

4) K_0 value

Coefficient of earth pressure at rest K_0 is assumed to be 0.5.

5) Plastic parameter G' in Eq.(11)
according to the study by Nishi and Esashi (1978), vaalue of G' is as follows.

$G'=192.3(\varphi'=38.4)$ loose sand
$G'=333.0(\varphi'=49.4)$ dense sand
$G'=250.0(\varphi'=42.4)$
$G'=192.0(\varphi'=33.6)$ gravel

using the above values, G' is calculated by the proportional allotment.

6) The other parameters used for calculations
Sand and Gravel
$M^*_m=1.108$, $M^*_f=1.279$, $\lambda=0.0098$, $\varkappa=0.003$

Clay
$M^* =1.2(=M^*_m)$, $M^* =1.4$ $C=2.0\times10^{-7}$ (1/sec)

$m'=28.0$, $\lambda= 0.091$, $\varkappa= 0.0087$

Input earthquake motion

The hypothetical earthquake which was proposed by Ozawa(1978) is used to obtain the incident wave motion. The magnitude is 6.8km and the epicenter is 6-11 km(Fig.1). The acceleration wave motion is obtained by the prediction model (level 2)of non-stationary earthquake motions proposed by Kameda et al.(1979). The N value in this prediction model is assumed to be 50, because we consider the incident wave at the base rock.

Numerical calculation and discussions

Numerical calculation and discussions

Figs.2and 4(sites 1-3) show the distribution of excess pore water pressure at sites 1-3 in the case that the amplitude of incident wave is 0.1 times as that of original hypothetical earthquake motion(Amp=0.1). In this case(Amp=0.1), the maximum values of acceleration at base rock are 12.4 gal(site 1), 15.2 gal(site 2) and 11.9 gal(site3). In any case, the excess pore water pressure is maximum near the surface. From Figs.2 and 4, it is evident that the excess pore water pressure is small in the clay layers at site 1 and site 3. However, at site 2, the excess pore water pressure is maximum in the clay layer near the surface. Then, we can conclude that liquefaction may occur in the soft clay layer near the surface.

When the amplitude of input earthquake motion is 0.5 times as that of original acceleration wave motion by non-stationary prediction model, liquefaction occurs in all layers after 16 sec in sites 1-3.

ACKNOWLEDGEMENT

The author wishes to thank Prof. H.Goto, Associate Prof. H. Kameda and Research assistant S.Sugito of Kyoto University for their support throughout of this study.

REFERENCES

Adachi, T. and F. Oka(1982),"Constitutive equations of normally consolidated clay based on elasto-viscoplasticity", Soils & Foundations, Vol.22, No.4,57-70.
Caquot, A. and J. Kerizel(1949),"Traite de Mechanique des sols", Gauthier-Villars,Paris.
Kameda, H.,M.Sugito and T. Asamura(1980)," Simulated earthquake motions scaled for magnitude, distance and local soil conditions", Proc. 7th WCEE, Vol.2,295-302
Kobori, T.(1978),"Prediction of dynamic characteristics of ground in Kyoto city and hazards estimation", Disater Prevention Council of Kyoto City,June.
Nishi, K. and Y. Esashi(1978),"Stress-strain relation of sand based on elasto-plasticity theory",Proc. of JSCE, No.280, Dec., 111-122.
Nishi, K. and Y. Esashi and H. Nakamura(1978), "The behaviour and design for large size intake pipes buriedin sea bed(part 3)", Report of Central Research Institute of Electric Power Industry, No.378004, 8-9.
Oka, F.(1981),"Prediction of time dependent behavior of clay", Proc. 9th ICSMFE,Vol.1, 215-218.
Oka, F. and K. Hibi(1982),"Liquefaction analysis of soil deposits composed of sands and clays", Proc. of Int. Symp. on Numerical Models in Geomechanics, Zurich,401-410.
Oka, F. and T. Murase(1980),"Liquefaction analysis of sand deposits based on cyclic elasto-plasticity",Proc. Int. Conf. on Recent Advances in Geotechnical Earthquake Engineering and Soil Dynamics, St. Louis, Vol.1, 151-154.

Oka, F. and K. Sekiguchi(1980),"Liquefaction analysis of horizontally layered sand considering a laterally confined condition Proc. 7th WCEE,Vol.3,125-128.

Oka, F. K. Sekiguchi and H. Goto(1981),"A method of analysis of earthquake-induced liquefaction of horizontally layered sand deposits",Soils& Foundations,Vol.21,1-17.

Oka, F. and H. Washizu(1981),"Constitutive equation for sands and overconsolidated clays under dynamic loads based on elasto-plasticity", Proc. of Int. Conf. on Recent Advances in Geotechnical Earthquake Engineering and Soil Dynamics, St. Louis,Vol.1,71-74.

Okubo, H. and M. Ogawa(1974),"Shear wave velocity of Osaka ground", 9th Proc. of Annual meeting of JSSMFE,725-728.

Ozawa, I.(1978),"Hypothetical earthquake for seismic hazards estimation for Kyoto City", Disaster Prevention Council of Kyoto City, June.

Sekiguchi, H. and H. Ohta(1977),"Induced anisotropy and time dependency in clays", Proc. Speciality session 9, 9th ICSCME, Tokyo,229-238.

Table II Weight per Unit Volume for Geomaterial

	Geomaterial	Weight per Volume gr/cm^3
Sand	Fine sand, Sandy Mud	1.7
	Fine sand, Sand containing shell	1.8
	Coarse sand	1.9
Clay	Silty clay	1.4
	Alluvial clay	1.5
	Diluvial clay	1.6
Gravel	Soft clay containing gravel	1.7
	clayey gravel	1.8
	Fine gravel	1.9
Rock and Mud stone		2.0

Table III Expected value of coefficent of permeability

Gravel	Sand		Fine sand Sandy Mud		Clay
10^2	1.0	10^{-2}	10^{-4}	10^{-6}	10^{-8}

k(cm/sec)

Table I Soil Parameters Profile

Site 1

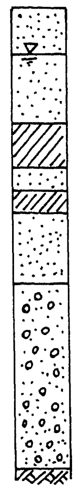

Depth	N	ρ	Vs	k	σ'_m	G'
0.0	1	183.67	67.80	10^{-5}	0.0	50.0
1.0	1	183.67	67.80	10^{-5}	0.120	50.0
2.0	1	183.67	67.80	10^{-5}	0.240	50.0
3.0	1	183.67	67.80	10^{-5}	0.293	50.0
4.0	1	183.67	67.80	10^{-5}	0.347	50.0
5.0	2	142.86	126.05	10^{-8}	0.387	50.0
6.0	2	142.86	126.05	10^{-8}	0.413	50.0
7.0	9	183.67	169.49	10^{-5}	0.453	85.0
8.0	9	142.86	213.39	10^{-8}	0.493	85.0
9.0	9	183.67	169.49	10^{-5}	0.533	85.0
10.0	9	183.67	169.49	10^{-5}	0.587	85.0
11.0	9	183.67	169.49	10^{-5}	0.640	85.0
12.0	33	193.88	289.58	10^{-3}	0.697	173.0
13.0	33	193.88	289.58	10^{-3}	0.757	173.0
14.0	33	193.88	289.58	10^{-3}	0.817	173.0
15.0	44	193.88	319.33	10^{-3}	0.877	215.0
16.0	44	193.88	319.33	10^{-3}	0.937	215.0
17.0	49	193.88	331.23	10^{-3}	0.997	234.0
18.0	49	193.88	331.23	10^{-3}	1.060	234.0
19.0	49	193.88	331.23	10^{-3}	1.120	234.0
20.0	49	234.00	600.00	10^{-3}	1.190	234.0

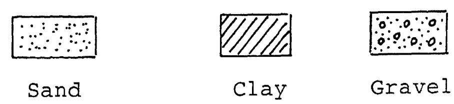

Site 2

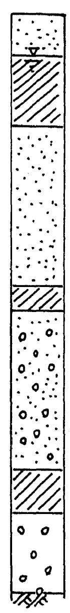

Depth	N	ρ	Vs	k	σ'_m	G'
0.0	12	183.67	191.09	10^{-5}	0.0	92.0
1.0	1	142.86	98.90	10^{-8}	0.107	50.0
2.0	1	142.86	98.90	10^{-8}	0.200	50.0
3.0	1	142.86	98.90	10^{-8}	0.227	50.0
4.0	1	142.86	98.90	10^{-8}	0.253	50.0
5.0	17	183.67	220.97	10^{-5}	0.293	111.0
6.0	17	183.67	220.97	10^{-5}	0.347	111.0
7.0	17	183.67	220.97	10^{-5}	0.400	111.0
8.0	17	183.67	220.97	10^{-5}	0.453	111.0
9.0	17	183.67	220.97	10^{-5}	0.507	111.0
10.0	17	183.67	220.97	10^{-5}	0.560	111.0
11.0	17	183.67	220.97	10^{-5}	0.613	111.0
12.0	8	142.86	204.78	10^{-7}	0.653	77.0
13.0	34	193.88	292.53	10^{-3}	0.697	177.0
14.0	34	193.88	292.53	10^{-3}	0.757	177.0
15.0	34	193.88	292.53	10^{-3}	0.817	177.0
16.0	34	193.88	292.53	10^{-3}	0.877	177.0
17.0	34	193.88	292.53	10^{-3}	0.937	177.0
18.0	34	193.88	292.53	10^{-3}	0.997	177.0
19.0	34	193.88	292.53	10^{-3}	1.060	177.0
20.0	10	142.86	221.41	10^{-8}	1.100	177.0
21.0	10	142.86	221.41	10^{-8}	1.130	177.0
22.0	40	193.88	309.15	10^{-3}	1.170	200.0
23.0	40	193.88	309.15	10^{-3}	1.230	200.0
24.0	40	193.88	309.15	10^{-3}	1.290	200.0
25.0	40	234.00	600.00	10^{-8}	1.360	200.0

Table I(Continued)

Site 3

Depth	N	ρ	Vs	k	σ'_m	G'
0.0	3	183.67	107.20	10^{-5}	0.0	50.0
1.0	3	183.67	107.20	10^{-5}	0.120	50.0
2.0	3	183.67	107.20	10^{-5}	0.240	50.0
3.0	3	183.67	107.20	10^{-5}	0.293	50.0
4.0	10	183.67	177.10	10^{-5}	0.347	85.0
5.0	10	183.67	177.10	10^{-5}	0.400	85.0
6.0	14	183.67	203.78	10^{-5}	0.453	100.0
7.0	14	183.67	203.78	10^{-5}	0.507	100.0
8.0	25	183.67	263.49	10^{-4}	0.560	142.0
9.0	22	183.67	263.49	10^{-4}	0.613	130.0
10.0	22	183.67	263.49	10^{-4}	0.667	130.0
11.0	5	153.06	263.49	10^{-8}	0.710	65.0
12.0	38	183.67	263.49	10^{-5}	0.753	200.0
13.0	4	153.06	263.49	10^{-8}	0.797	60.0
14.0	42	183.67	263.49	10^{-3}	0.840	207.0
15.0	47	183.67	263.49	10^{-3}	0.893	227.0
16.0	47	183.67	263.49	10^{-3}	0.947	227.0
17.0	50	193.88	263.49	10^{-3}	1.000	250.0
18.0	50	193.88	263.49	10^{-3}	1.060	250.0
19.0	50	193.88	263.49	10^{-3}	1.120	250.0
20.0	50	234.00	263.49	10^{-8}	1.200	250.0

Depth(m), N(Blow-count), ρ(mass density, $Kgf/m^4/sec^2$), V_s(shear wave velocity, m/sec), k(permeability coefficient, m/sec), σ'_m($x10^4$ kgf/m^2)

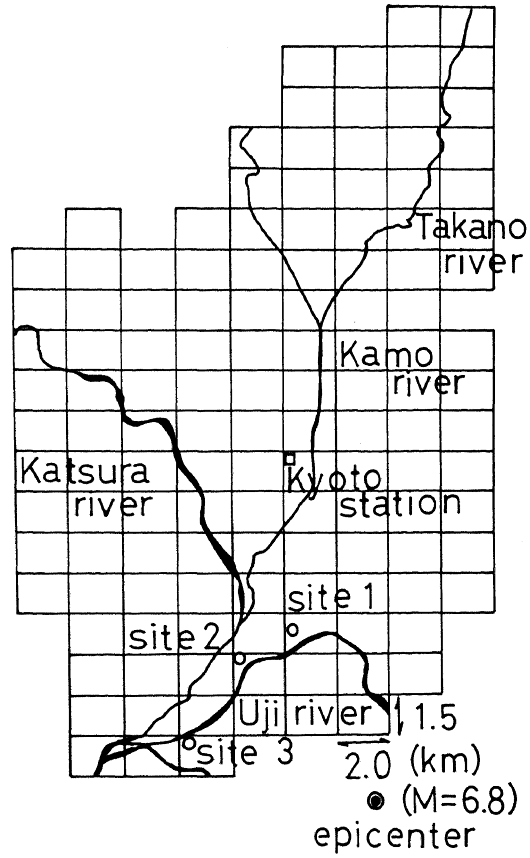

Fig.1 Hypothetical Earthquake in Kyoto City

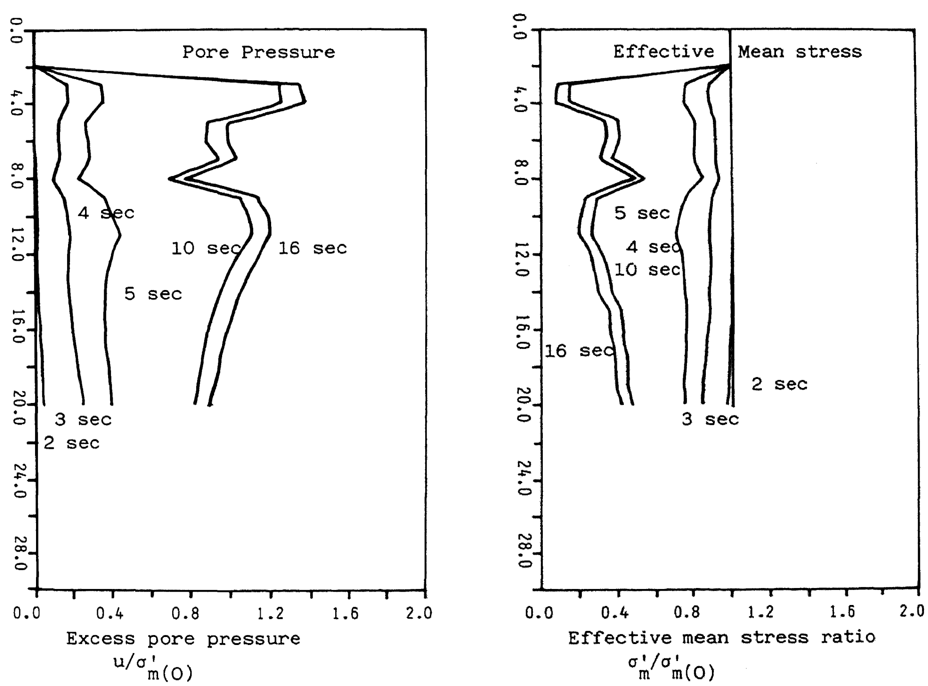

Fig.2 Distributions of excess pore water pressure and mean effective stress(Site 1, Amp=0.1)

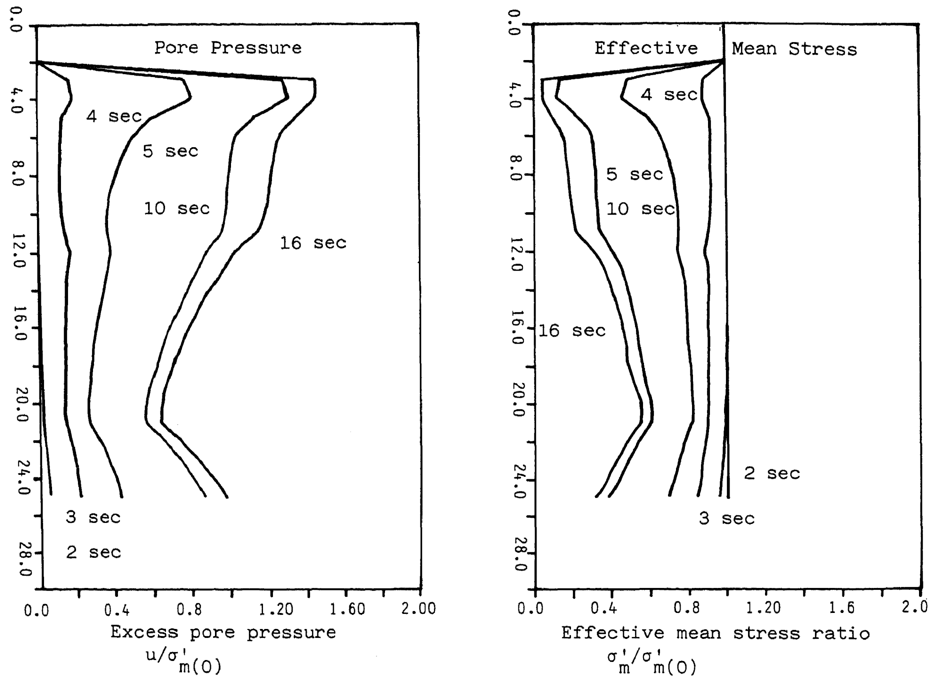

Fig.3 Distributions of excess pore water pressure and mean effective stress(Site 2, Amp=0.1)

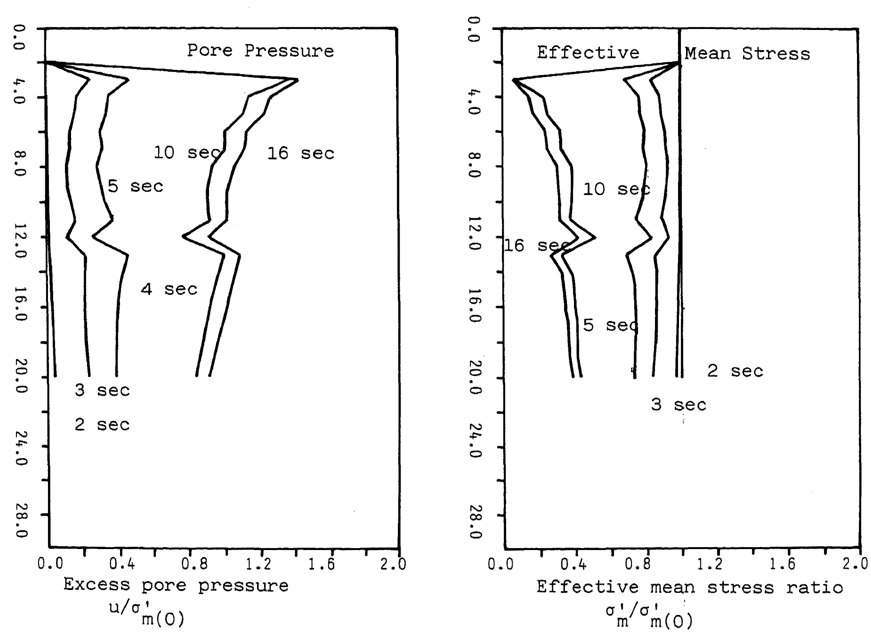

Fig.4 Distributions of excess pore water pressure and mean effective stress(Site 3, Amp=0.1)